AD-A080 426 NATIONAL WEATHER SERVICE SILVER SPRING MD TECHNIQUES --ETC F/G 17/7
NOWCASTS AND SHORT-RANGE (0-2 HOUR) FORECASTS OF THUNDERSTORMS --ETC(U)
NOV 79 M A ALAKA, R C ELVANDER, R E SAFFLE DOT-FA78WAI-886
UNCLASSIFIED FAA-RD-79-98 NL

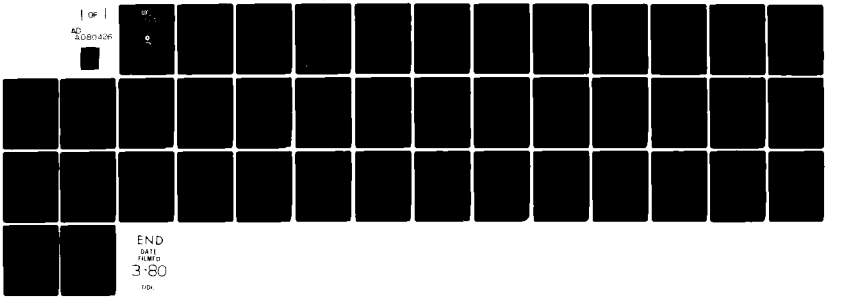

END
DATE FILMED
3-80
DDC

(18) (19) Report No. FAA-RD 79-98

LEVEL II

(12)

(6)

NOWCASTS AND SHORT-RANGE (Ø-2 HOUR) FORECASTS OF THUNDERSTORMS AND SEVERE CONVECTIVE WEATHER FOR USE IN AIR TRAFFIC CONTROL.

(10) Mikhail A./Alaka, Robert C./Elvander, Robert E./Saffle
Techniques Development Laboratory
Systems Development Office
National Weather Service

(12) 41

(11) Nov 79
(9) FINAL REPORT. Apr 78 - Nov 79,

(15) DOT-FA78WA1-[illegible]
Prepared for
U.S. DEPARTMENT OF TRANSPORTATION
FEDERAL AVIATION ADMINISTRATION
Systems Research & Development Service
Washington, D.C. 20590

8

407 167

NOTICE

This document is disseminated under the sponsorship of the Department of Transportation in the interest of information exchange. The United States Government assumes no liability for its contents or use thereof.

Technical Report Documentation Page

1. Report No.	2. Government Accession No.	3. Recipient's Catalog No.
FAA-RD-79 - 98		

4. Title and Subtitle	5. Report Date
NOWCASTS AND SHORT-RANGE (0-2 HOUR) FORECASTS OF THUNDERSTORMS AND SEVERE CONVECTIVE WEATHER FOR USE IN AIR TRAFFIC CONTROL.	September 1979
	6. Performing Organization Code
7. Author(s)	8. Performing Organization Report No.
M.A. Alaka, R.C. Elvander, and R.E. Saffle	
9. Performing Organization Name and Address	10. Work Unit No. (TRAIS)
U.S. Department of Commerce, NOAA National Weather Service 8060 13th Street Silver Spring, Md. 20910	152-461-01
	11. Contract or Grant No. Interagency Agreement DOT/FA78WAI-886
12. Sponsoring Agency Name and Address	13. Type of Report and Period Covered
U.S. Department of Transportation Federal Aviation Administration Systems Research & Development Service, Sys. Dev. Div. Aviation Weather Branch, Washington, D.C. 20591	Final Report April 1978 - November 1979
	14. Sponsoring Agency Code FAA/ARD-410

15. Supplementary Notes

Prepared under FAA Interagency Agreement No. DOT/AF78WAI-886, managed by the Aviation Weather Branch, ARD-410.

16. Abstract

Since 1971, weather radars with automatic signal digitizing capability have been undergoing operational testing and evaluation as part of the Digitized Radar Experiment (D/RADEX) of the National Weather Service. The data generated by these radars have been used to develop automated techniques for monitoring and predicting thunderstorms and severe local convective weather at or near air terminals.

Digital radar data, archived over a period of six years, have been used in conjunction with a sophisticated technique to identify and track each important echo within the radar umbrella. Parameters based on reflectivities, echo tops, and the estimated vertically-integrated liquid-water (VIL) have been computed for each echo and statistically related to the reported severe weather occurrences. The derived relationship can be used to estimate the probability of a given cell being associated with severe weather.

In the predictive part of the effort, the objective is to forecast the locations and intensity of convective weather activity for periods of up to 1 hour. We have derived statistical equations relating various radar-based parameters to subsequently observed radar reflectivity values. The parameters used involve observed and extrapolated patterns of reflectivities, echo tops, and VIL. The system movement vector used for extrapolating the radar fields is objectively determined by binary matching of successive observations of reflectivity patterns.

17. Key Words	18. Distribution Statement
Short-Range Forecasting Probability of Severe Weather Digital Radar Data Applications	Document is available to the U.S. public through the National Technical Information Service, Springfield Virginia 22151

19. Security Classif. (of this report)	20. Security Classif. (of this page)	21. No. of Pages	22. Price
Unclassified	Unclassified	42	

Form DOT F 1700.7 (8-72) Reproduction of completed page authorized

PREFACE

The authors thank Frank Lewis for discussions concerning the implications of the results of this study, and Peggy A. Gardner for typing this manuscript.

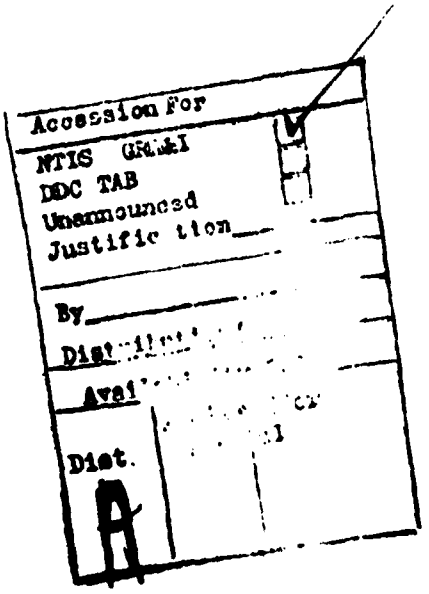

METRIC CONVERSION FACTORS

Approximate Conversions to Metric Measures

Symbol	When You Know	Multiply by	To Find	Symbol
		LENGTH		
in	inches	*2.5	centimeters	cm
ft	feet	30	centimeters	cm
yd	yards	0.9	meters	m
mi	miles	1.6	kilometers	km
		AREA		
in^2	square inches	6.5	square centimeters	cm^2
ft^2	square feet	0.09	*square meters*	m^2
yd^2	square yards	*0.8*	*square meters*	m^2
mi^2	square miles	2.6	square kilometers	km^2
	acres	*0.4*	hectares	ha
		MASS (weight)		
oz	ounces	28	grams	g
lb	pounds	0.45	kilograms	kg
	short tons (2000 lb)	0.9	tonnes	t
		VOLUME		
tsp	teaspoons	5	milliliters	ml
Tbsp	tablespoons	15	milliliters	ml
fl oz	fluid ounces	30	*milliliters*	ml
c	cups	0.24	liters	*l*
pt	pints	0.47	liters	l
qt	quarts	0.95	liters	l
gal	gallons	*3.8*	*liters*	l
ft^3	cubic feet	*0.03*	*cubic meters*	m^3
yd^3	cubic yards	0.76	cubic meters	m^3
		TEMPERATURE (exact)		
°F	Fahrenheit temperature	5/9 (after subtracting 32)	Celsius temperature	°C

*1 in = 2.54 (exactly). *For other exact conversions and more detailed tables, see NBS Misc. Publ. 286, Units of Weights and Measures.* Price $2.25, SD Catalog No. C13.10:286.

Approximate Conversions from Metric Measures

Symbol	When You Know	Multiply by	To Find	Symbol
		LENGTH		
mm	millimeters	0.04	inches	in
cm	centimeters	0.4	inches	in
m	meters	3.3	feet	ft
m	meters	1.1	yards	yd
km	kilometers	0.6	miles	mi
		AREA		
cm^2	square centimeters	0.16	square inches	in^2
m^2	square meters	1.2	square yards	yd^2
km^2	square kilometers	0.4	square miles	mi^2
ha	hectares (10,000 m^2)	2.5	acres	
		MASS (weight)		
g	*grams*	0.035	ounces	oz
kg	kilograms	2.2	pounds	lb
t	tonnes (1000 kg)	1.1	short tons	
		VOLUME		
ml	milliliters	0.03	fluid ounces	fl oz
l	liters	2.1	pints	pt
l	liters	1.06	quarts	qt
l	*liters*	0.26	gallons	gal
m^3	*cubic meters*	35	cubic feet	ft^3
m^3	cubic meters	1.3	cubic yards	yd^3
		TEMPERATURE (exact)		
°C	Celsius temperature	9/5 (then add 32)	Fahrenheit temperature	°F

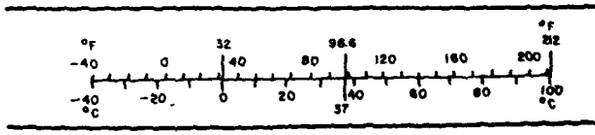

TABLE OF CONTENTS

LIST OF ILLUSTRATIONS

LIST OF TABLES

LIST OF ABBREVIATIONS

A/D = Analog to digital converter

AFOS = Automation of Field Operations and Services

CSI = Critical success index

dbz = Decibel measure of radar reflectivity

D/RADEX = Digitized radar experiment

FAR = False alarm ratio

NOAA = National Oceanic and Atmospheric Administration

NSSFC = National Severe Storms Forecast Center

NSSL = National Severe Storms Laboratory

NWS = National Weather Service

POD = Probability of detection

PPI = Plan position indicator

RADAP = Radar data processor

TDL = Techniques Development Laboratory

TOPS = Echo top heights

VIL = Vertically-integrated liquid water content

VIP = Video integrator and processor

WSR = Weather search radar

Z = Radar reflectivity (mm^6/m^3)

ZTR = Zero tilt reflectivity

NOWCASTS AND SHORT-RANGE (0-2 HOUR) FORECASTS OF THUNDERSTORMS AND SEVERE CONVECTIVE WEATHER FOR USE IN AIR TRAFFIC CONTROL

1.0 Introduction

This report deals with a continued effort by the Techniques Development Laboratory (TDL) of the National Weather Service (NWS) to develop, for the benefit of aviation, improved automated techniques for monitoring and forecasting thunderstorms and severe local convective weather at and around air terminals. Products developed under this effort are intended primarily for air traffic controllers who are in direct contact with the pilots. They need detailed weather information to plan deviation requests and, when possible, to give avoidance advisories to aircraft under their control. They are, therefore, most interested in current hazardous weather conditions (NOWCASTS*) and the changes likely to occur within the time range of 10 minutes to 2 hours (FORECASTS).

One of the most effective ways of determining, with sufficient timeliness and detail, the location, movement, and evolution of convective weather is to monitor the radar echoes associated with them. Therefore, observations from WSR-57 radars constitute our main data base. Serious consideration was given to the use of other types of data such as observations from satellites, surface observations, and output from numerical models. However, these data sources were discarded due to their lack of timeliness and difficulty of aquisition. These problems may be overcome in the future when Automation of Field Operations and Services (AFOS) or another similar system becomes operational.

2.0 Nowcasts

Perhaps the most important weather information required by pilots and air traffic controllers is the current distribution and intensity of strong convective cells and their associated phenomena. These include heavy showers, thunderstorms, large hail, gusty winds, strong wind shear, and tornadoes. Weather radars offer the best means of monitoring the location of these cells and measuring their intensity. The National Weather Service operates a network of weather radars located primarily in the eastern two thirds of the United States.

Currently, radar observations are made manually. Three main operational procedures are available for transmitting information from NWS to the users:

a. Once per hour, a radar operator encodes the maximum zero tilt reflectivity (ZTR), categorized into 6 levels by a Video Integrator and Processor (VIP), on a rectangular grid surrounding the radar site. He

---

* For the purpose of this report, a NOWCAST is defined as a description of current weather, without any forecast implication.

then adds notations concerning maximum echo top heights, movements of echoes, and special features, such as hook echoes. The combined information is transmitted to the NWS central computer facility where it is merged with reports from other sites to produce a national facsimile for field users. This product is of limited use to air traffic controllers because of the coarseness of the grid (about 22 n mi mesh length) and the large time lag between observations and product dissemination.

b. During periods of significant weather, the operator monitors the radar continuously for special features that might indicate the presence of severe weather. Upon observing such a feature, he can telephone alert or warning information to forecasters or directly to the public safety agencies in the affected area. Here, too, specialized service is not provided for air traffic controllers unless the operator identifies a potential severe weather cell approaching an airport.

c. Finally, facsimile recording devices are available which allow a user to dial into a desired radar and receive a gray-shades-on-paper reproduction of the latest radar base-elevation PPI (plan position indicator) display. Such a product would also include radar operator notations concerning maximum echo tops heights, echo movement, hook echoes, etc. However, the reproduction quality is often poor, and the special remarks are dependent on the operator for updating.

2.1 D/RADEX and RADAP

In 1971, the NWS initiated project D/RADEX (Digitized Radar Experiment) to test the feasibility of using minicomputers to process digitized radar data into useful meteorological products in near real-time (McGrew, 1972). The D/RADEX system originally consisted of a network of four WSR 57 radars equipped with minicomputers. They were located at Okalahoma City, Okla., Monett, Mo., Kansas City, Mo., and Stephenville, Tex. Later, an additional unit in Pittsburg, Pa. was added to the network and the one in Stephenville was discontinued.

After several years of experimentation, the NWS concluded that a nationwide system of digitized radars with minicomputer capabilities was highly desirable. Accordingly, the NWS has decided to install, over the next few years, a Radar Data Processor (RADAP) at each site in the National radar network. Each RADAP will include a minicomputer, color graphic and alphanumeric display devices, and communication ports. Thus RADAP will essentially be an expanded, operational version of D/RADEX.

Under the RADAP system, the processing and transmitting of digitized radar data will be largely automatic. In addition to benefits such as continual monitoring and faster response times, RADAP will produce a fundamental change in the type of radar data transmitted. Today's radar products are concerned mainly with what can be termed "raw" data such as reflectivity, height of echo tops, and movement of echoes. The user of the data (forecaster, controller, etc.) must somehow transform this information into forecasts of echo activity and assessments of severe weather potential. Analysis techniques are often subjective and thus vary in quality depending on the skill and experience of a particular user. Also, they are frequently

time consuming. Thus, in periods of widespread, significant convective activity, it becomes difficult to give all areas proper attention. Under RADAP, objective techniques can be developed that will generate products more directly related to the weather. This is the capability that we intend to exploit to provide weather data to the air traffic controller.

RADAP will not be in place for several years. Meanwhile, the D/RADEX network offers an interim means to develop and evaluate radar data processing techniques that are aimed for RADAP implementation.

The NWS categorizes the analog type radar reflectivities into six levels for PPI display. These are usually called VIP levels because the categorization can be done automatically by the Video Integrator and Processor. The reflectivity thresholds (minimum power returned values) of these categories are given in Table 1. In D/RADEX, analog reflectivity values are digitized by an analog to digitial converter (A/D). These are then categorized into 10 intensity levels from 0-9. The reflectivity thresholds of these levels are also given in Table 1. The D/RADEX levels were designed to give finer resolution than VIP levels at low rainfall rates and at intensities indicating the possibility of hail. Six D/RADEX levels were forced to coincide with VIP levels in order to display reflectivity maps in values familiar to users. D/RADEX intensity levels are recorded for 1 n mi by 2° bins on each even azimuth over the entire range from 10 n mi through 125 n mi. These observations, archived on magnetic tape, form the base from which specification and forecast techniques can be developed. In D/RADEX operations, the data must be converted into a cartesian grid for mapped products. In doing so, the maximum reflectivity found in any given box is assigned to that box.

2.2 Current D/RADEX Products

As described by Saffle (1976), D/RADEX already generates several products that could be useful for air traffic control. One of these is a gridded map of current base-elevation reflectivity intensities (Figure 1). The intensities are coded into six VIP levels whose power returned thresholds are given in Table 1. This product is updated every 10 minutes and can be transmitted to an airport control tower within two minutes of observation time*. Minimum threshold values can be specified so that only significant intensities would be transmitted. For initial testing, we have designed a program to generate gridded reflectivity maps covering the airport area with areal resolution of 1 n mi by 2 n mi. With this product, a controller would have continually updated information on current convective activity in his airport area, displayed with high areal resolution. The information can be easily interpreted and is capable of being displayed at any specified level of significance. Figure 2 illustrates this product.

---

* A goal for future air traffic control operations is a two-minute update of VIP-level displays.

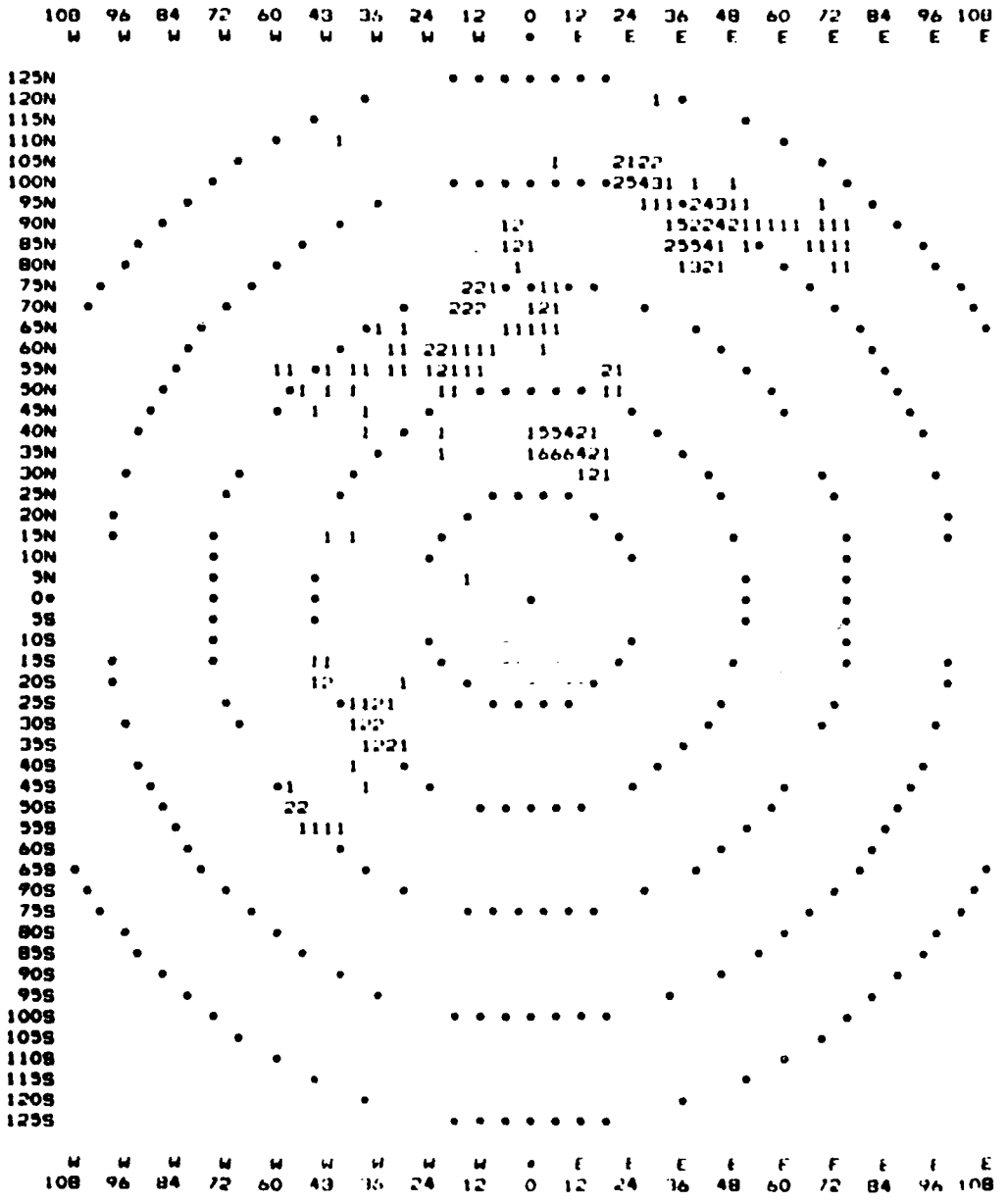

Figure 1. Mapped VIP values indicating the ZTR intensities of echoes. Coordinates show distance in n mi north, south, east, and west of radar location. The resolution of each grid box is 3 n mi east-west by 5 n mi north-south. Distance between range markers is 25 n mi.

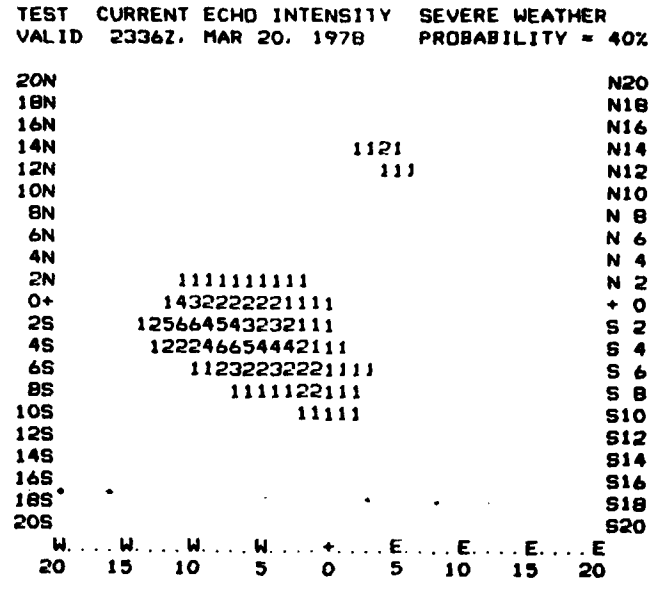

Figure 2. Mapped VIP values indicating the current ZTR intensities over a terminal area. The resolution of each grid box is 1 n mi east-west by 2 n mi north-south. Also shown is the objectively estimated probability of severe weather of the strongest cell in the area.

Table 1. Reflectivity Threshold for VIP and D/RADEX levels.

VIP LEVEL	D/RADEX LEVEL	REFLECTIVITY THRESHOLD (dbz)
1*	1	18.5
	2	24.5
2	3	30.0
	4	34.0
3	5	41.0
4	6	46.0
5	7	51.0
6	8	57.0
	9	62.0

*level 1's are close but not exactly comparable.

Besides maps of ZTR, D/RADEX also computes several products intended to depict the vertical structure of a cell. These products require multi-elevation scans of reflectivity. Twice per hour, D/RADEX takes consecutive scans at 2° increments of antenna elevation until no echoes are observed. There are experimental plans to increase the frequency of these observations to three times per hour. The first product developed from tilt data was a grid map of estimated echo top heights (TOPS) (Figure 3). This provides more information on echo top heights than can be determined from the two or three maximum tops currently reported from the operator's manual observation.

After Greene (1972) published his work on relating vertically integrated liquid water content (VIL) to severe weather, a program was developed under D/RADEX to compute such a product from tilt data sequences. VIL maps tie together on one display information concerning the reflectivity at all levels of the vertical development of cells (Figure 4). VIL is calculated from the formula:

$$VIL = \sum_{i=1}^{n} 3.44 \times 10^{-6} \left(\frac{Z_i + Z_{i+1}}{2} \right)^{4/7} \partial h$$

Where:

VIL is given in kg of water per square meter of surface area,

Z_i = reflectivity at level i,

n = number of height increments through the vertical extent of the echo,

$\partial h = h_{i+1} - h_i$ = difference between two consecutive levels.

Since water has a density approximately equal to one, VIL can be considered as the depth of water per unit area, that is a VIL of 25 means there are 25 mm of water in the echo above that unit area.

Recently, Lemon (1977) has brought together and quantized some ideas about the relationship to severe weather of cells whose reflectivity cores tilt back into the steering wind field. The area below the echo overhang is called a weak echo region (WER). Identifying WER cells manually requires the operator to sweep the radar beam back and forth across each candidate cell at different elevation angles--a time consuming process when several cells exist. With D/RADEX, we have developed a product that first uses VIL values to identify strong cells and then uses tilt data to map low- and mid-level fields for all chosen cells. The two fields are displayed together by assigning the letter H to grid boxes with mid-level echo only, the letter L to grid boxes with low-level echo only, and the low level reflectivity VIP value to those grid boxes having an echo at both levels (Figure 5). With such displays, Lemon's criteria can be checked for many cells in a short time.

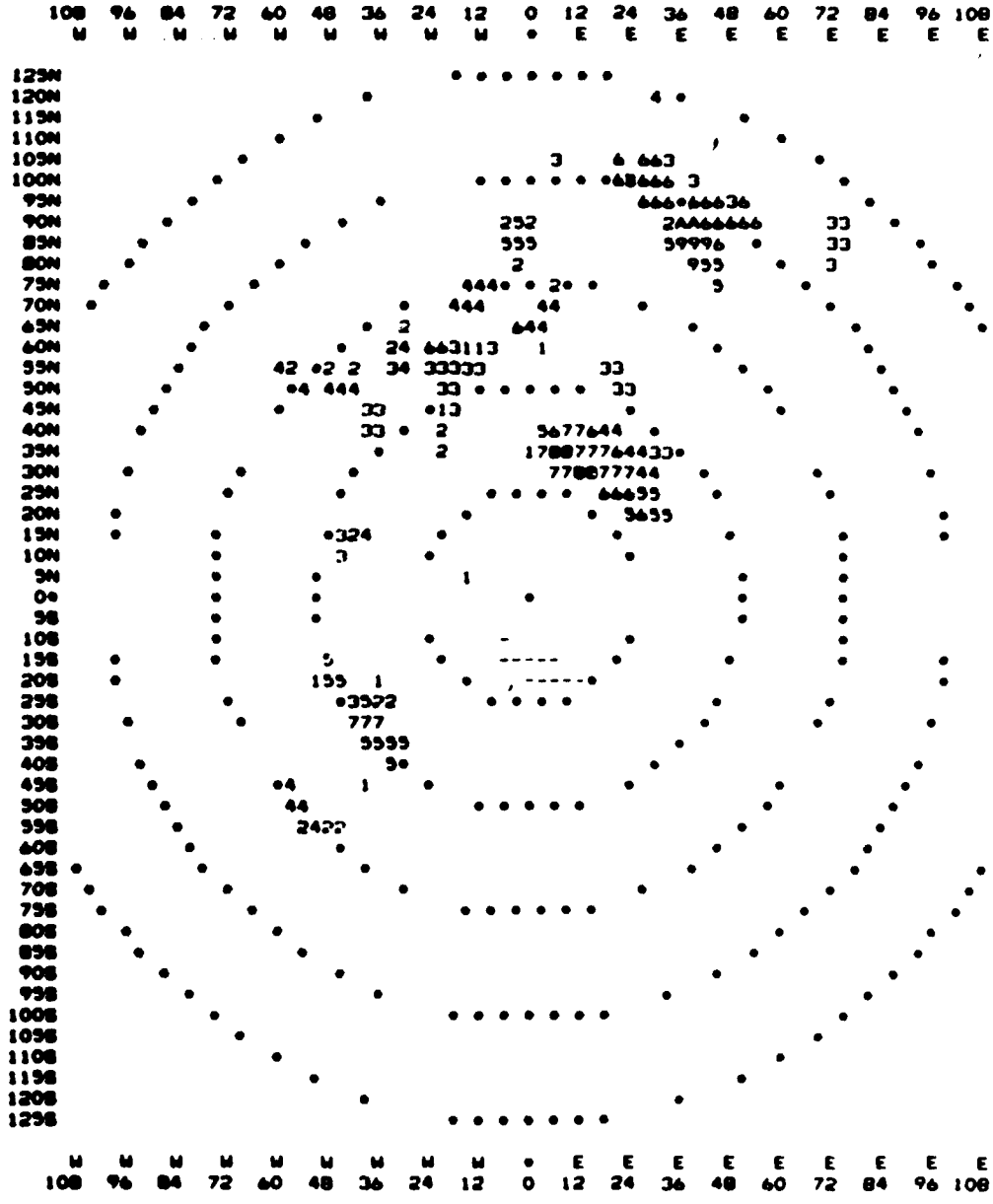

Figure 3. Mapped code value indicating the height of echoes shown in Figure 1. Code values are given for 5000 ft categories of height; values 1, 2, . . ., 9, A, . . . E represent heights of 5000, 10000, . . . 45000, 50000, . . ., 70000 ft respectively.

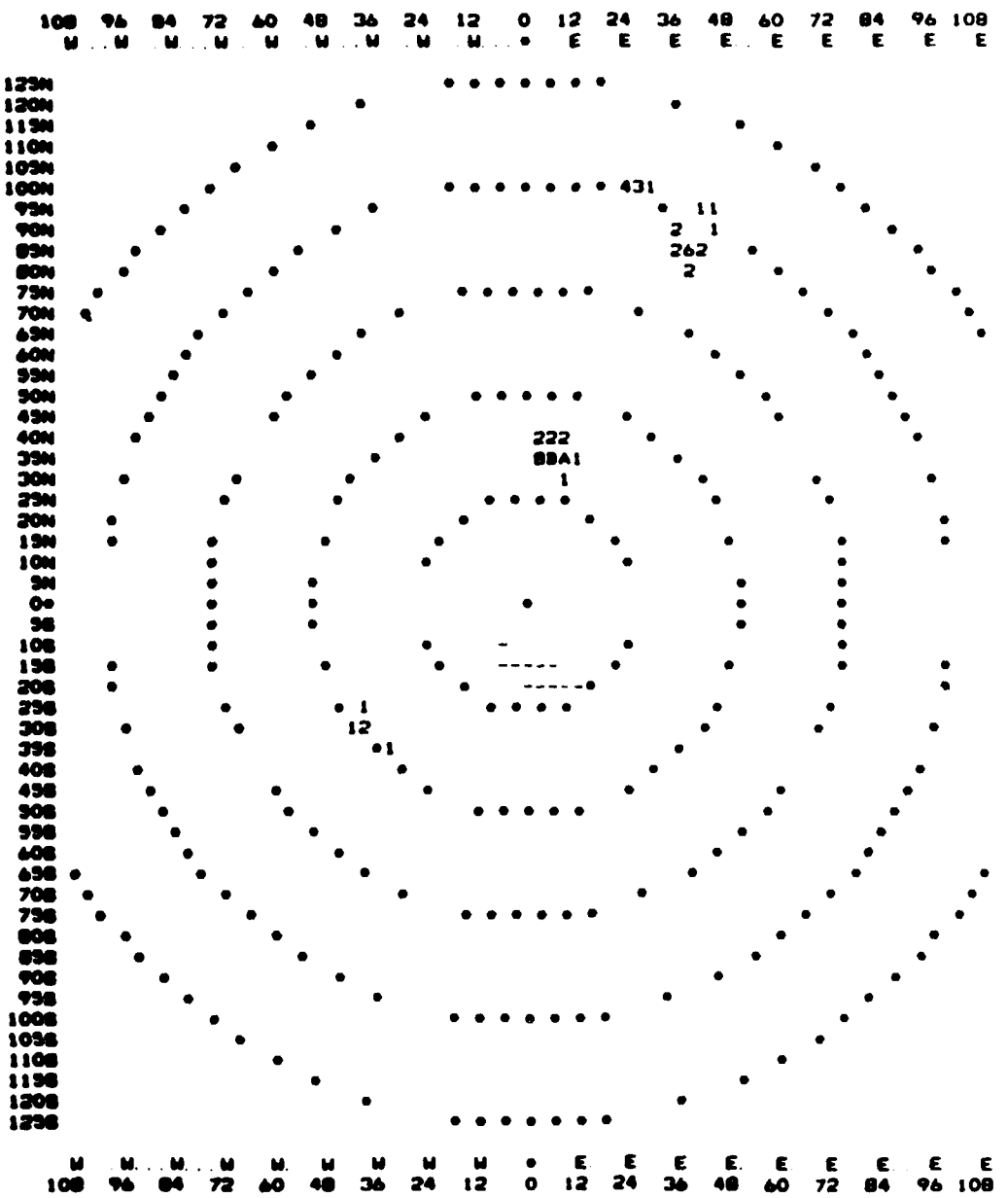

Figure 4. Mapped code values indicating the vertically integrated liquid water (VIL) of echoes shown in Figure 1. Codes 1, 2, . . . 9, A, . . . G correspond to VIL of 5, 10, . . . 45, 50, . . . 80 respectively.

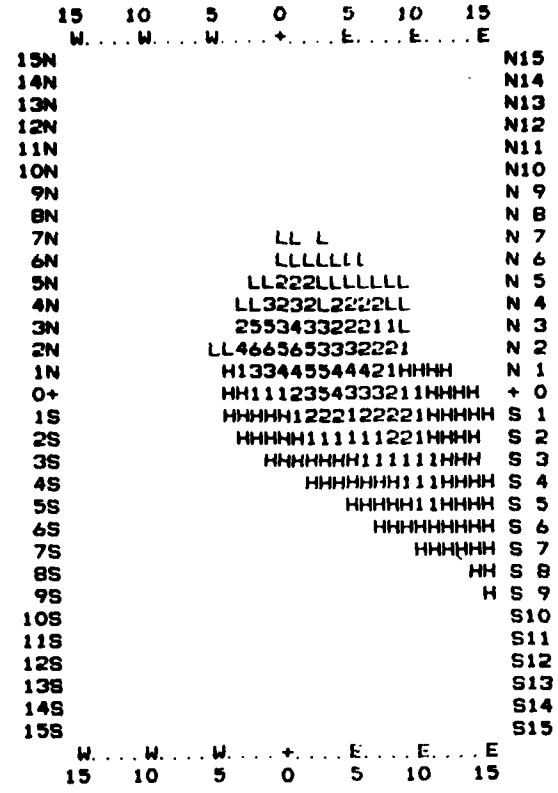

Figure 5. High areal resolution (1 n mi by 1 n mi) display of a thunderstorm cell. Cell tilt with altitude is shown by using L's and H's to indicate areas with echoes at low level (4000 - 8000 ft) or high level (28000 - 32000 ft) only. In areas with echoes at both levels, the low level VIP is printed to give intensity information and to give a position from which to measure echo overhang. In this case 3 n mi of overhang can be seen on the right flank of the storm as well as a considerable amount of anvil downstream from the storm's centroid.

The products discussed above are intended mainly as guidance to meteorologists concerned with severe weather forecasting. Of the three, only TOPS would have direct application to general aviation. Also, experimentation is needed to determine how many weather products can be properly assimilated by the controller. Effective use of some data fields at the airport terminal would require a meteorologist for analysis and interpretation.

2.3 Identifying Potentially Severe Weather Cells

We now have the capacity to perform real-time computations which reveal the potential severity of thunderstorm cells within the radar umbrella. To this end, we have used digitized radar data, archived at the National Severe Storms Laboratory (NSSL) for the years 1969-71 and 1973-74. These data are in essentially the same format as the D/RADEX data discussed earlier. The main difference is that the reflectivity thresholds corresponding to digits 1 through 9, although constant throughout each collection period, may vary from one episode to another. This was done in order to adjust the digits to the range of reflectivities expected in a given storm. In this way, the maximum reflectivity resolution possible was attained for different classes of storms. Thus, the reflectivities associated with the NSSL digits are not directly comparable to the D/RADEX digits shown in Table 1.

We used the base-tilt data for our ZTR reflectivity parameters and developed cartesian plots of VIL values from the tilt sequences of reflectivity estimates, using a program originally developed by Greene (1972). The data were stored after the scan conversion routines in 60 x 60 square arrays of 4 n mi grid length.

2.3.1 Echo Isolation

We have employed a contour tracing method to identify individual echoes. Points on the grid which have an intensity less than a predetermined threshold value are temporarily set to zero. Directed line segments from one zero element to another define echo boundaries. However, to avoid excessive fragmentation of some large echoes, if an element greater than a threshold value R is connected to another by one (but not more than one) element of value R-1, then the entire mass is considered an echo.

In a previous study, Elvander (1976) studied the relationship between the occurrence of severe weather and the intensity of ZTR and VIL fields, using the 1972 archived NSSL data. Echoes were manually isolated and tracked over a series of consecutive observations--an extremely time-consuming procedure. Maximum ZTR and VIL values of echoes, and echo sizes with ZTR values larger than VIP3 were related to reports of severe weather. Results with ZTR data confirmed previous studies by Wilson (1971) and Brandes (1972) that both echo size and high reflectivity are pertinent factors in determining its probable association with severe weather.

On the basis of these results, we have attempted to isolate potentially significant ZTR echoes by applying a significance weight (SWT) criterion combined with an intensity threshold equivalent to VIP3. This was found by Elvander (1977) to be a good discriminator between cells associated with severe weather and those which are not.

The SWT, a dimensionless number ranging from 0 to 600, was originally defined by Blackmer et al (1973). It combines maximum reflectivity and echo size and thus imposes a selectivity constraint since only echoes which are either intense, or large, or both, are selected for further consideration. The trade-off between maximum intensity within the cell and

the size of the cell was discussed by Alaka et al (1975). The SWT will be further discussed in section 2.3.4 below.

In the present study, only ZTR echoes with a reflectivity threshold of VIP3 (or slightly less) and a SWT of 250 or more were considered. Table 2 shows the number of ZTR cells obtained by applying this reflectivity threshold in conjunction with different SWT threshold values. It also shows the number and percentage of cells in each category associated with severe weather events. As expected, the higher the SWT value, the greater the likelihood that the cell is associated with severe weather.

Table 2. Number of ZTR cells obtained by applying a minimum intensity threshold of VIP3 in conjunction with different SWT values, and their association with severe weather (s/w).

SWT	>250	>300	>350	>400	>450
Number of cells	1220	932	610	302	128
Number with s/w	130	119	106	77	50
Percentage with s/w	10.7	12.8	17.7	25.5	39.1

The criterion for defining VIL-based cells was the existence of at least two adjacent grid boxes with VIL values of 10 or more. From five years of data (1969-71 and 1973-74), we defined 474 cells. These form the basic VIL data set. Table 3 shows the distribution of VIL cells when different threshold VIL values are applied, and the number and percentage of the cells in each category associated with severe weather. Again, as expected, the percentage of cells with severe weather increases gradually as the VIL criterion is raised.

2.3.2 Statistical Procedure

We have used a multiple screening regression technique (Miller, 1958) to determine the degree of assocation of severe convective weather with different echo configurations. The approach depends on the collection of a statistically significant sample of candidate predictors derived from digitized radar data, and a corresponding sample of reported occurrences of the predictand. The probability of occurrence of the predictand is expressed in terms of a weighted linear combination of the predictors selected by the screening process. The first predictor selected has the highest individual correlation with the predictand. The second predictor, together with the first, gives the greatest multiple correlation coefficient or reduction of variance. The screening process is repeated until a predetermined number of predictors are selected, or until the reduction of variance by additional predictors goes down to a predetermined lower limit.

Table 3. Number of VIL cells obtained by applying different threshold criteria, and the degree of their association with severe weather (s/w).

VIL threshold	All Cells	>15	>20	>25	>30
Number of Cells	474	400	316	255	193
Number of s/w	87	81	71	65	53
Percentage with s/w	18.4	20.3	22.5	25.5	27.5

2.3.3 The Predictand Data Sample

The predictand data consisted of reports of tornadoes or funnel clouds, surface hail $\geq$ 3/4 in ($\sim$ 2 cm), and wind gust $\geq$ 50 kt ($\sim$ 93 km/hr) and/or wind damage. The reports were obtained from the Environmental Data Service publication "Storm Data", from the severe storm tapes of the National Severe Storms Forecast Center (NSSFC), and from the volunteer observer network of NSSL. All of these reports were scrutinized to eliminate any identifiable errors such as redundant, misplotted, or false reports.

2.3.4 Predictors

2.3.4.1 ZTR Predictors

The various predictors developed from the ZTR data sample are listed in Table 4.

Predictor 1 is the number of grid boxes covered by the cell. Typically, larger cells are more likely to be associated with severe weather than smaller cells. Predictor 2 is the average reflectivity of the cell. Predictors 3, 4, and 5, are the number of grid boxes with reflectivity digits equal to or exceeding NWS VIP levels 3, 4, and 5 respectively. Predictors 6, 7, and 8 are reflectivity weighted echo sizes (echo masses) with reflectivities equal to or greater than VIP level 3, 4, and 5 respectively.

Predictors 9, 10, 11 represent different ways to rate small, intense cells in comparison with large, relatively weak cells. Significance weight SWT combines the maximum reflectivity and the sum of the estimated (Marshall - Palmer) rainfall rates in the cell; it provides a trade-off between cell intensity and size. The main factors in predictor WTB are the summed reflectivity and maximum intensity. If a cell is large and intense, subtracting the log of the cell size is unimportant. However, if it is

Table 4. Predictors derived from zero tilt reflectivity (ZTR) data.

1.	ZTR SIZE	Number of grid boxes (N) covered by echo.
2.	AVGZ	$\sum_{i=k}^{9} N(Z_i)Z_i/N$; k is the reflectivity threshold
3.	SGEV3	$\sum_{i=k}^{9} N(Z_i)$; $Z_k \geq$ VIP3
4.	SGEV4	$\sum_{i=k}^{9} N(Z_i)$; $Z_k \geq$ VIP4
5.	SGEV5	$\sum_{i=k}^{9} N(Z_i)$; $Z_k \geq$ VIP5
6.	MGEV3	$\sum_{i=k}^{9} N(Z_i)Z_i$; $Z_k \geq$ VIP3
7.	MGEV4	$\sum_{i=k}^{9} N(Z_i)Z_i$; $Z_k \geq$ VIP4
8.	MGEV5	$\sum_{i=k}^{9} N(Z_i)Z_i$; $Z_k \geq$ VIP5
9.	SWT	$100 \log\left[(Z_{max}/100)^{1/2} (\Sigma Z/100)^{1/1.6}\right]$
10.	WTB	$10\left[Z_{max}\log_{10}(\Sigma Z) - \log_{10}N\right]$
11.	WTD	$100 \log_{10}(N^{1/2}\Sigma Z)$
12.	SUMPAR	$\sum_{i=2}^{5} N(VIP_i \leq Z \leq VIP_{i+1})Z(VIP_{i+1})$
13.	BIN 250	1 if SWT > 250, 0 otherwise
14.	BIN 300	1 if SWT > 300, 0 otherwise
15.	BIN 350	1 if SWT > 350, 0 otherwise
16.	BIN 400	1 if SWT > 400, 0 otherwise
17.	BIN 450	1 if SWT > 450, 0 otherwise

large and weak, the predictor value will be reduced. Predictor WTD multiples the size of the cell by the summed reflectivities. It again provides an equivalence between small intense cells and larger but weaker ones.

Predictor 12 is similar to predictors 6, 7, and 8 but considers the total mass of the echo.

Finally, predictors 13-17 are binary values of SWT. Earlier studies have shown these to be good discriminators of severe weather.

Table 5 lists the linear correlations between ZTR predictors and the occurrence of severe weather for the different data groupings of Table 2. In general, the most highly correlated predictors are those which combine echo size and intensity. These predictors tend to retain their relative ranking although, in general, their correlation with severe weather tends to decrease as the SWT threshold is raised.

2.3.4.2 VIL Predictors

Table 6 reveals an interesting relationship between the life span of ZTR cells and the occurrence of severe weather. Cells with lifetimes of more than 30 minutes have a 20.2 percent chance of being associated with severe weather, while in shorter lived cells, the probability is considerably less. In view of this relationship, we have included the lifetime of cells among the VIL predictors in Table 7.

The predictors developed from the VIL data sample are listed in Table 7. They are mostly self-explanatory. Predictor 2 (MAX VIL) is the maximum VIL value observed in the cell at the time of the severe weather event, or at the time of max VIL WGT if no severe weather occurred. VIL WGT is the maximum VIL value (V_{max}), assigned to a group of boxes with values ranging from V_{max} to V_{max-4}, times the number of boxes N containing these values. In VIL MASS, the grid box VIL values contained in a cell are sorted out into groups with VIL values ranging from i+1 to i+5, i.e, 6-10, 11-15, 16-20, etc. The number of boxes in these groups is then respectively multiplied by 2, 3, 4, etc. and summed up.

Table 8 lists the linear correlations between severe weather and VIL predictors, computed from the data groupings of Table 3. Note that the correlations are typically higher than those of the ZTR predictors and tend to retain their value or, in the case of the continuous predictors, to increase as the threshold criterion is raised. Again, the predictors with the highest correlation coefficients (VIL WGT and VIL MASS) combine echo mass and intensity.

2.4 Results from Screening Regressions

We have applied multiple screening regressions to different combinations of the data sets and subsets listed in Tables 2 and 3. We shall now give some of the results obtained. We divided the results into three

Table 5. Linear correlations between each ZTR predictor and severe weather events - based on the ZTR data set.

	Data Sets				
Predictor	All Cells	SWT >300	SWT >350	SWT >400	SWT >450
ZTR SIZE	.317	.308	.280	.239	.174
AVGZ	.122	.106	.074	.035	-.053
SGEV3	.305	.299	.270	.234	.147
SGEV4	.160	.159	.150	.246	.155
SGEV5	.238	.232	.204	.163	.047
MGEV3	.292	.288	.264	.237	.133
MGEV4	.235	.232	.213	.183	.082
SUMPAR	.307	.301	.271	.238	.128
SWT	.319	.335	.313	.314	.205
WTB	.291	.288	.251	.257	.094
WTD	.321	.335	.317	.312	.237
BIN 250	.014	-	-	-	-
BIN 300	.123	-	-	-	-
BIN 350	.218	.190	-	-	-
BIN 400	.276	.264	.212	-	-
BIN 450	.315	.314	.295	.267	-
Number of cells	1220	932	610	302	.128
Number with Severe Weather	130	119	106	77	50

main groups, namely, those obtained from: a) ZTR predictors alone, b) VIL predictors alone, and c) joint ZTR/VIL predictors. In each case, a lower limit of 1 percent reduction of variance was used as a criterion in the selection of predictors. In the cases discussed below, P denotes the probability of occurrence of the predictand, R.V. is the reduction of variance, and S.E. is the standard error of estimate.

Table 6. Distribution of cells according to their life span and their association with severe weather (s/w).

Lifetime	Number of Cells	Number with s/w	% with s/w
$\leq$ 10 min.	358	10	2.8
$\leq$ 20 min.	541	17	3.1
$\leq$ 30 min.	699	25	3.6
> 30 min.	521	105	20.2
Total	1220	130	10.7

Table 7. Predictors derived from vertically integrated liquid water content data.

Predictors	Definition
1. VIL SIZE	Number of grid boxes (N) covered by echo
2. MAX VIL	V_{max}
3. VIL WGT	$N(V_{max})$
4. v. MASS	$\Sigma N[VIL(i+1) - VIL\frac{(i+5)}{5}](i+1)$; i = 5, 10, ... 100
5. SVG10	Size (N) of echo having VIL > 10
6. SVG15	Size (N) of echo having VIL > 15
7. SVG20	Size (N) of echo having VIL > 20
8. SVG25	Size (N) of echo having VIL > 25
9. BIN15	1 if VIL > 15, 0 otherwise
10. BIN20	1 if VIL > 20, 0 otherwise
11. BIN25	1 if VIL > 25, 0 otherwise
12. BIN30	1 if VIL > 30, 0 otherwise
13. BIN35	1 if VIL > 35, 0 otherwise
14. BIN40	1 if VIL > 40, 0 otherwise
15. BIN45	1 if VIL > 45, 0 otherwise
16. LIFETIME	Lifetime of VIL cell

Table 8. Linear correlations between each VIL predictor and severe weather events - based on the VIL data set.

	Data Sets				
Predictor	All Cells	VIL >15	VIL >20	VIL >25	VIL >30
VIL SIZE	.344	.343	.352	.328	.337
MAX VIL	.344	.343	.358	.346	.400
VIL WGT	.349	.349	.360	.350	.372
VIL MASS	.365	.365	.377	.360	.382
SVG10	.336	.334	.344	.321	.337
SVG15	.333	.328	.335	.317	.346
SVG20	.339	.336	.346	.330	.350
SVG25	.338	.335	.344	.331	.360
BIN 15	.114	-	-	-	-
BIN 20	.150	.107	-	-	-
BIN 25	.199	.173	.148	-	-
BIN 30	.195	.173	.150	.080	-
BIN 35	.211	.194	.178	.129	.116
BIN 40	.231	.218	.209	.173	.175
BIN 45	.223	.212	.204	.174	.173
LIFETIME	.250	.243	.221	.215	.202
Number of Cells	474	400	316	255	193
Number with severe weather	87	81	71	65	53

2.4.1 Results from ZTR Predictors

The regression equations for estimating the probability of severe weather in a given cell, for the different data groupings listed in Table 2 are:

Case 1. SWT $\bar{>}$ 250; 1220 cells

$$P = -.383 + (8.41 \times 10^{-4})WTD + (.185)BIN450$$

R.V. = 12.2% S.E. = .290

Case 2. SWT > 300; 932 cells

$$P = -.583 + (1.84 \times 10^{-3})SWT + (1.47 \times 10^{-3})SGEV4$$

R.V. = 12.3% S.E. = .313

Case 3. SWT > 350; 610 cells

$P = -1.13 + (2.10 \times 10^{-3})WTD + (1.39 \times 10^{-3})SGEV4$

R.V. = 11.2% S.E. = .358

Case 4. SWT > 400; 302 cells

$P = -1.83 + (4.73 \times 10^{-3})SWT - (1.71 \times 10^{-2})SGEV5$

R.V. = 11.1% S.E. = .474

Case 5. SWT > 450; 128 cells

$P = -3.36 + (5.51 \times 10^{-3})WTD - (1.99 \times 10^{-2})SGEV5$

R.V. = 8.2% S.E. = .475

Although the observed frequency of severe weather events increases from 10.7 percent to 39.1 between case 1 and case 5, the first predictor selected in all five cases is a significance weight predictor. And, excluding case 1 the second predictor selected is the size of the cell with reflectivity equal to or greater than the NWS VIP 4 or 5 levels. These results demonstrate well the importance of size and intensity of ZTR cells for severe weather occurrence. Note that the standard errors of estimate increase as the data set is made more restrictive. This is partly due to the larger variance of the predictand, as the SWT is made larger. Since the predictand is a binary variable, the variance is approximately equal to p(1-p), where p is the observed frequency. In case 1, p = .107, hence the variance is (.107) x (.893) = .096. In case 5, on the other hand, p = .391 and the variance p(1-p) = .238. Therefore, since the reductions of variance do not increase dramatically, the standard errors of estimate increase as the SWT threshold is raised. For the first four cases the reductions in variance range from 11 to 12 percent, and it is only 8 percent in case 5. Note the consequent larger standard error in case 5.

2.4.2 Results from VIL Predictors Alone

A selection of the regression equations obtained from the VIL predictors is given below:

Case 6. VIL > 10; 474 cells

$P = 0.33 + (7.56 \times 10^{-3})VIL\ MASS - (4.13 \times 10^{-2})SVG15 + (1.16 \times 10^{-2})LIFETIME$

R.V. = 15.9% S.E. = .357

Case 7. VIL > 15; 400 cells

$$P = .047 + (8.48 \times 10^{-3})\text{VIL MASS} - (5.01 \times 10^{-2})\text{SVG15} + (1.10 \times 10^{-2})\text{LIFETIME}$$

R.V. = 16.5% S.E. = .370

Case 8. VIL > 20; 316 cells

$$P = .081 + (9.76 \times 10^{-3})\text{VIL MASS} - (5.83 \times 10^{-2})\text{SVG15}$$

R.V. = 17.0% S.E. = .383

Case 9. VIL > 25; 255 cells

$$P = .098 + (1.01 \times 10^{-2})\text{VIL MASS} - (6.29 \times 10^{-2})\text{SVG15}$$

R.V. = 16.1% S.E. = .402

Case 10. VIL > 30; 193 cells

$$P = -.295 + (1.06 \times 10^{-2})\text{VIL MASS} - (2.32 \times 10^{-1})\text{BIN 45} + (5.41 \times 10^{-3})\text{VIL SIZE} + (9.66 \times 10^{-3})\text{LIFETIME}$$

R.V. = 22.0% S.E. = .402

In general, probabilities developed from VIL predictors account for a higher reduction of variance than those based on ZTR data alone. Values range from 16.5 to 22.0 percent. The standard error of about 0.35 to 0.4 is high in comparison with that of 0.21 found by Elvander (1977) when he applied a threshold VIL value of 5 to the 1972 NSSL data. Typically, the standard error increases with the threshold value.

In all the cases computed with VIL predictors, the VIL MASS was selected first. In the first four cases, SVG15 was the second predictor selected. LIFETIME was selected third in three cases out of five. The results again emphasize the importance of echo size (and longevity) to the development of severe convective weather.

2.4.3 Results Using Joint ZTR/VIL Predictors

In another set of experiments, we ran screening regressions on data sets composed of both ZTR and VIL predictors. For the purpose of this experiment, we defined ZTR cells corresponding to the VIL cells previously defined. However, we experienced some difficulty because the ZTR cell was often not at its maximum intensity at the same time as the VIL cell, and frequently several VIL cells, some having severe weather, others not, were related to one large ZTR cell. This combination of events led to poor correlations between severe weather and the ZTR predictors in the joint ZTR/VIL data set. Therefore, results were almost identical to those obtained from the previous set of experiments in which only VIL predictors were used, and we shall not discuss them further. However, we must note that an important disadvantage of using ZTR data is that they typically define large, intense cells in which the precise location of severe weather is hard to determine. On the other hand, VIL cells are typically smaller, and the placement of possible severe weather associated with them is more easily accomplished.

2.4.4 Verification on Dependent Data

We have verified the probability estimates of severe weather on the dependent data, using the equations shown in case 6-10. Only VIL predictors were used in these equations. We divided the estimated probabilities into groups of ten percent, ie., 0 - 10 - 20, etc., and compared these with the actual frequencies observed for those deciles. Such a figure is called a reliability diagram.

Figure 6 illustrates the performance of the equation derived in case 6, when the entire VIL data sample was used. The number of events in each decile is enclosed in parentheses. The relationship is almost linear indicating the equation is reliable, i.e., high estimates of probability have high frequencies of occurrence. The reliability curves for the equations derived in case 7 - 10 are similar, indicating the derivations are reasonable and useful.

Another way to describe the value of the equations, and the division of the data sets as well, is by means of the threat score, or Critical Success Index (CSI) (Donaldson, et al 1975). Other related scores are the Probability of Detection (POD) and the False Alarm Ratio (FAR). Table 9 describes the necessary information to compute these scores. A successful forecast (X) occurs when the forecast verifies, a miss (Y) when an event not forecasted occurs, and a false alarm (Z) when a forecast event does not occur. Cases of forecasting no event correctly (W) aren't considered here.

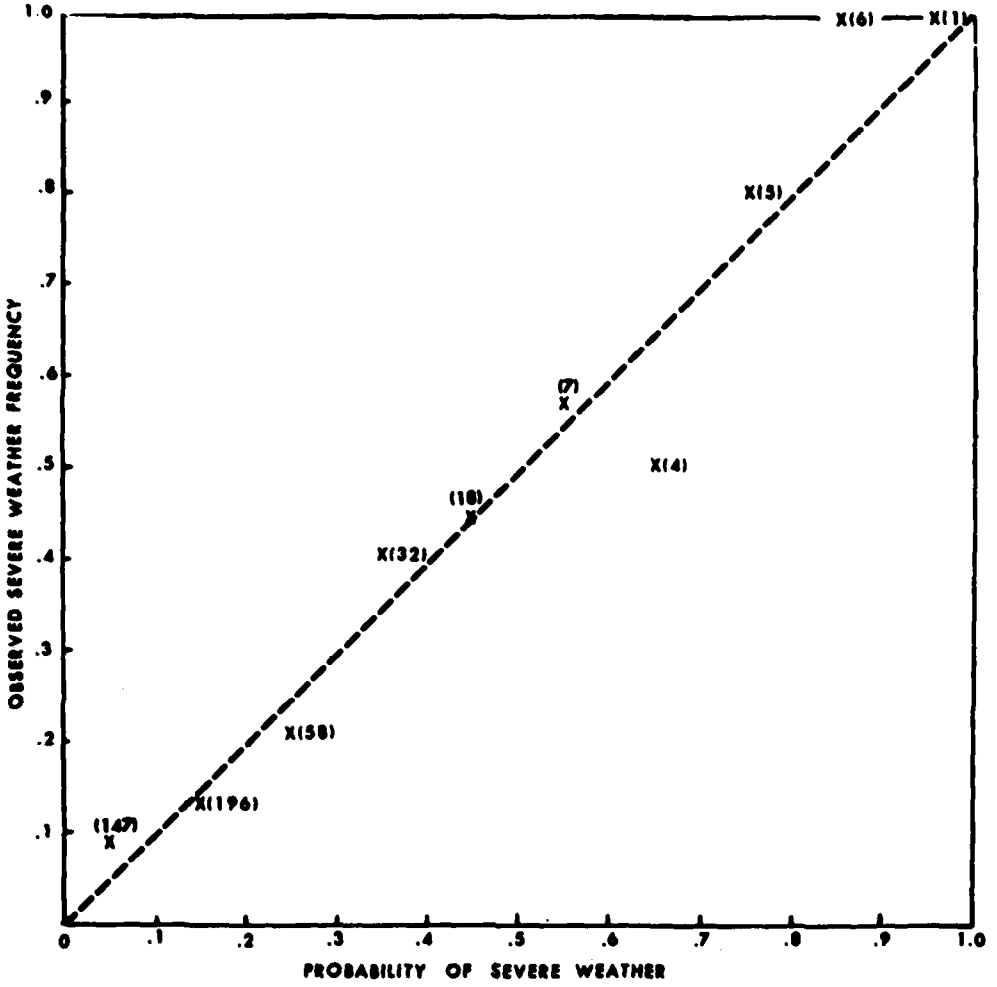

Figure 6. Relationship between the observed frequency of severe weather producing cells for deciles of estimates of the probability of severe weather, based on the equation listed in case 6. The numbers in parentheses are the total numbers of cells in each decile. The diagonal line represents a perfect one-to-one relationship.

Following are the scores used and their definitions:

a. Probability of Detection (POD) described by Donaldson et al (1975), also referred to by Panofsky and Brier (1958) as prefigurance.

$$POD = X/(X + Y)$$

Table 9. Contingency table defining the variables used in computing the verification scores.

	Forecast	
Observed	Occurrence of Severe Weather	Non-Occurrence of Severe Weather
Occurrence of Severe Weather	X	Y
Non-Occurrence of Severe Weather	Z	W

b. False Alarm Ratio (FAR): (1 - postagreement)

$$FAR = Z/(X + Z)$$

c. Critical Success Index (CSI), formerly known as the 'threat score' (Palmer and Allen (1964).

$$CSI = X/(X + Y + Z)$$

It is interesting to compute these scores for the basic data sets described in Tables 2 and 3. In the collection of storm reports in Storm Data and the NSSFC severe weather tape, we found 14 events during the data collection to which we could not associate a ZTR cell. On the other hand, 246 reports were related to 130 cells. Table 10 lists the CSI, POD, and FAR scores attainable by using the SWT thresholds alone as categorical identifiers of severe weather. We have assumed that each report not associated with a ZTR cell, 14 in all, is a miss.

As the SWT criterion is raised, the CSI score increases. However, the number of events missed also increases. When a SWT of 450 is used, 80 of the 130 severe weather producing cells are not accounted for. On the other hand, when all the data are used, ie., SWT equal to or greater than 250, the FAR score is almost equal to the POD! The table illustrates the major problem of forecasting rare events: to forecast correctly most of the occurrences, one must expect a relatively large number of false alarms.

The skill scores computed from the VIL data set and subset are listed in Table 11. We were able to relate 146 severe weather reports to the 87 VIL cells having severe weather; 13 additional reports could not be related to a VIL cell as defined in this study (two adjacent gridboxes having VIL values of 10 or more). As before, we have assumed reports not associated with a cell to be "misses".

Table 10. Performance of the ZTR cells, grouped according to SWT thresholds, as categorical identifiers of severe weather.

SWT Threshold	Number of Cells/Number with Severe Weather	CSI	POD	FAR
250	1220/130	.105	.903	.893
300	932/119	.124	.826	.872
350	610/106	.164	.736	.836
450	128/50	.225	.347	.609

Table 11. Performance of the VIL cells, grouped according to VIL thresholds, as categorical identifiers of severe weather.

VIL Threshold	Number of cells/Number with Severe Weather	CSI	POD	FAR
10	474/87	.179	.870	.816
15	400/81	.193	.810	.798
20	316/71	.206	.710	.775
25	255/65	.224	.650	.745
30	193/53	.221	.530	.725

A maximum CSI score of .224 is attained in the data group containing only those cells having values greater than 25. This value is almost the same as that found for the ZTR group having SWT greater than 450, which was .225. However, 53 percent of the severe weather producing cells are contained in the VIL group, whereas only 34.7 percent are contained in the ZTR group. On the other hand, the FAR score is larger for the VIL group (.745, vs .609). The large false alarm ratio is a major difficulty with severe weather forecasts. One of the problems may be inadequate reporting of severe weather types, hail, and wind. Burgess et al. (1979) estimate that only about 12 percent of these reports are contained in the Storm Data publication (and consequently on the NSSFC data tapes), because the damage is less than the $50,000 minimum required for inclusion.

We have made some initial attempts to verfy the forecast equations by means of CSI and associated scores. To do this, we have to form categorical forecasts of severe weather. This is done by assigning "Yes" values to probability estimates equal to or greater than 0.1, 0.2, etc. Probability estimates less than the selected value are assigned a "No". We found that the maxima in CSI scores for these categorical forecasts were obtained with probability of 0.2 to 0.3 for the equations derived in cases 6 - 10.

A CSI score of 0.271 was obtained for case 6 when a categorical value of 0.20 was used. Similar values were found for the other equations and the POD was 0.490. The score of 0.271 is an improvement over the

value of 0.179 obtained by using the VIL cell definition as a Yes/No forecast (note Table 12), but only half the severe weather producing cells are included in the sample.

We have constructed another graph which we believe emphasizes the utility of the equations. We have plotted the percentage of severe weather cells having probability estimates equal to or greater than the categorical values as a function of these values. Figure 7 illustrates the results. Again, an approximately linear relationship is noticeable. However, in this case there is a shift (bias) of about 0.20 toward the observed frequencies. This figure, along with the reliability graph discussed earlier, illustrates that the equations do perform adequately on the dependent data. Tests in the field, on independent data, will demonstrate their ultimate worth.

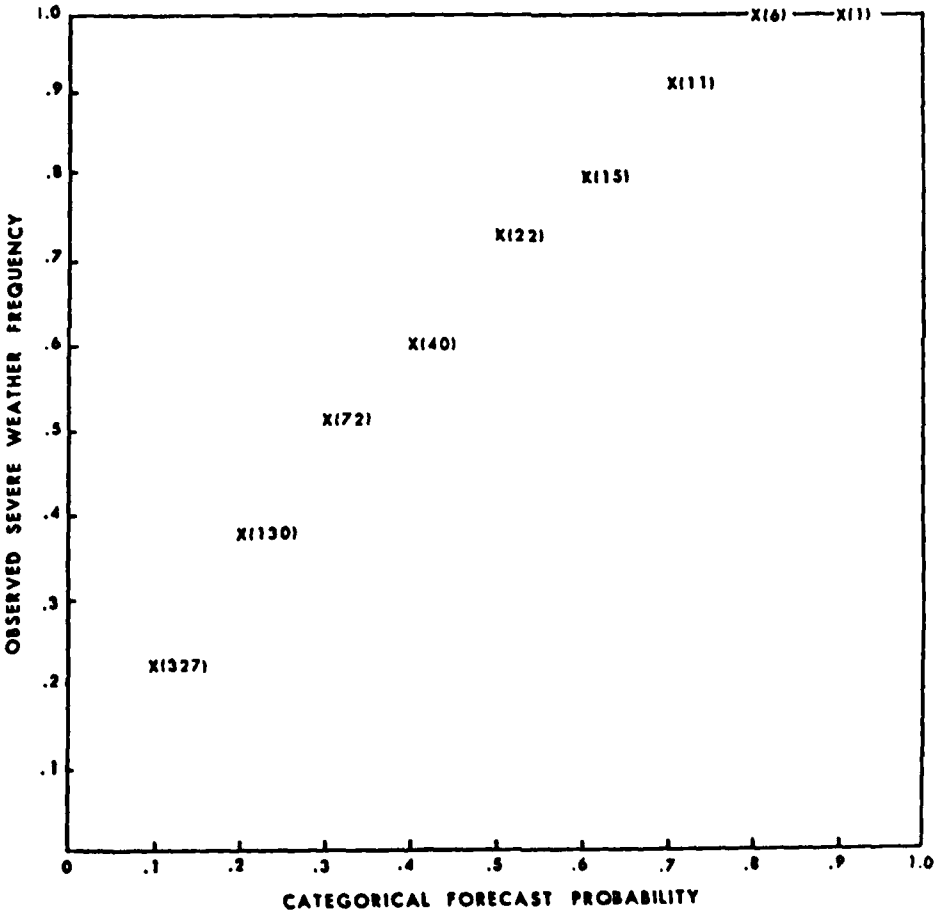

Figure 7. Relationship between the categorical (Yes/No) probability of severe weather estimates based on the equation listed in case 6, and the observed frequency of severe weather producing cells having probability estimates equal to or greater than the categorical value. The numbers in parentheses are the total number of cells having probability estimates equal to or larger than the categorical estimate.

3.0 Forecasts

In addition to displays of current convective weather, the controller requires forecasts of echo locations and intensities for time periods up to 2 h. Reliable forecasts will enhance the ability of the controllers to plan for efficient and safe use of terminal airspace.

3.1 Procedure

We used multiple linear regression analysis to derive equations relating parameters calculated from digitized radar data to subsequent observations of ZTR values. Our data base consisted of D/RADEX data from Oklahoma City in May and June of 1976. We decided that our candidate predictors would be based mainly on the gridded products already available under D/RADEX, i.e., maps of ZTR, TOPS, and VIL. The resolution of the grid boxes in these maps is 3 n mi east-west by 5 n mi north-south. Other types of meteorological data (satellite, surface observations, model output, etc.) were not considered due to the difficulty in obtaining them for real-time application at the radar sites.

As input to the regression program, a first set of parameters was designed to reveal the predictive value of persistence. These predictors were the observed ZTR, TOPS, and VIL. However, since the motion of echoes is very important for short range forecasting, we also included ZTR, TOPS, and VIL values extrapolated forward to the desired forecast valid time. In order to evaluate the relative merits of high areal resolution, coarse areal resolution, and areal smoothing, we used as separate predictors the individual grid box values of the parameters, the parameters' maximum values over 9 adjacent grid boxes, and their average values over 9 grid boxes. All of these parameters are objective, quickly calculable on minicomputers, and representative of all available radar data.

The motion vector used for extrapolating the predictor fields was a simplified version of the technique of cross-correlation of consecutive echo patterns developed by Austin and Bellon (1974). Rather than compute cross-correlation coefficients, we used a binary match technique. This consists of displacing one scan's echo pattern a varying amount in all directions, overlaying each shifted pattern with the next scan's observed pattern, and counting the number of grid boxes with non-zero ZTR in both. The displacement producing the largest number of matching boxes is used to calculate a motion vector for the time interval between the two scans. A series of such vectors is summed over an hour to produce a system movement vector (SMV). This type of motion vector is easily programmed and runs very quickly on a minicomputer.

Elvander (1976) compared the accuracy of the above technique with other more complex techniques. For the general class of convective weather, he found little difference in skill among these techniques. In additional, unreported work, Elvander found little deterioration in skill in our system movement vector as compared to the original technique of Austin and Bellon.

Two special parameters were designed to evaluate the predictive value of the past tendency of a cell to grow or decay. This was done by replacing ZTR values of the latest two scans by their 9-box average and maximum values. The earlier scan was then extrapolated by our system movement vector and the corresponding grid-box values compared. The difference (plus or minus) was then added to the latest observed maximum and average grid-box values, and the resultant values extrapolated forward to the forecast valid time. Thus, if the trend of a particular cell was to grow, its extrapolated value was also increased. Also, time of day was offered as a potential predictor to see whether diurnal influences would be important for very short range forecasts.

Tables 12 and 13 list the candidate predictors based on ZTR and tilt sequence data respectively.

Table 12. Candidate Predictors Calculated from ZTR Data.

1. ZOBX - the currently observed ZTR value in each grid box.
2. ZOMX - the maximum ZOBX over 9 adjacent grid boxes.
3. ZOAV - the average ZOBX over 9 adjacent grid boxes.
4. ZPBX - ZOBX extrapolated to the forecast valid time.
5. ZPMX - ZOMX extrapolated to the forecast valid time.
6. ZPAV - ZOAV extrapolated to the forecast valid time.
7. ZTMX - the trend (increase or decrease) in ZOMX over the previous 12 min.
8. ZTAV - the trend (increase or decrease) in ZOAV over the previous 12 min.
9. TOD - the hour of the day.

3.2 Results

We derived forecast equations for 12 min and 36 min projections. Separate equations were derived from ZTR predictors only and from joint ZTR and tilt sequence predictors. However, the predictand in both cases was the ZTR value in any given grid box. The reason for developing the two separate sets of equations was not only to find out the relative merits of the two

Table 13. Candidate Predictors Calculated from TILT Data.

1. TOBX - the latest observed maximum TOPS value in each grid box.
2. TOMX - the maximum TOBX over 9 adjacent grid boxes.
3. TOAV - the average TOBX over 9 adjacent grid boxes.
4. TPBX - TOBX extrapolated to the forecast valid time.
5. TPMX - TOMX extrapolated to the forecast valid time.
6. TPAV - TOAV extrapolated to the forecast valid time.
7. VOBX - the latest observed maximum VIL value in each grid box.
8. VOMX - the maximum VOBX over 9 adjacent grid boxes.
9. VOAV - the average VOBX over 9 adjacent grid boxes.
10. VPBX - VOBX extrapolated to the forecast valid time.
11. VPMX - VOMX extrapolated to the forecast valid time.
12. VPAV - VOAV extrapolated to the forecast valid time.

predictor sets, but also to develop back up equations for situations when tilt data sequences were not available. A low-limit criterion of 1 percent reduction of variance was again used in the selection of predictors. Results, based on 700 sets of observations covering two months, were as follows:

a. Projection = 12 min; Predictors = ZTR only

Forecast ZTR = -.01 + (.40)ZPAV + (.31)ZTAV + (.23)ZPBX

R.V. = 68% S.E. = .94

b. Projection = 12 min; Predictors = ZTR + Tilt

Forecast ZTR = -.10 + (.35)ZPAV + (.05)TPAV + (.30)ZTAV

R.V. = 71% S.E. = .88

c. Projection = 36 min; Predictors = ZTR only

Forecast ZTR = .18 + (.45)ZPAV + (.04)TOD

R.V. = 39% S.E. = 1.3

d. Projection = 36 min; Predictors = ZTR + Tilt

Forecast ZTR = .06 + (.13)TPAV

R.V. = 68% S.E. = .95

In evaluating the above results, we considered three main factors: a)whether our equations showed any appreciable skill, b) how much this skill deteriorated with length of forecast projection, and c) the types of predictors best correlated with subsequent ZTR patterns.

The reduction of variance and standard error associated with 12 min forecast projections show a considerable level of skill. This skill level drops when ZTR predictors only are used to make 36 min forecasts, but is maintained when joint ZTR and tilt sequence predictors are used. Also, tilt predictors were the only ones picked from the combined ZTR and tilt sequence predictors for the 36 min projections. For both forecast projections, the most effective predictors are extrapolations of 9-box averaged parameters. Figure 8 is an example of a 36 min forecast.

4.0 Future work

Severe weather probability and convective weather forecasting equations derived in the course of the present effort will be tested in an operational environment to evaluate controller/pilot response and to design proper display formats. A systematic verification of the equations will be made on independent data collected at D/RADEX sites in 1979 and 1980. In addition, the data base will be expanded to include D/RADEX data from Oklahoma City, Okla., Stephenville, Tex., Monett, Mo., and Pittsburg, Pa., for the years 1976 through 1978. Serious consideration will be given to the use of new parameters derived from Doppler radar velocity data and other sources.

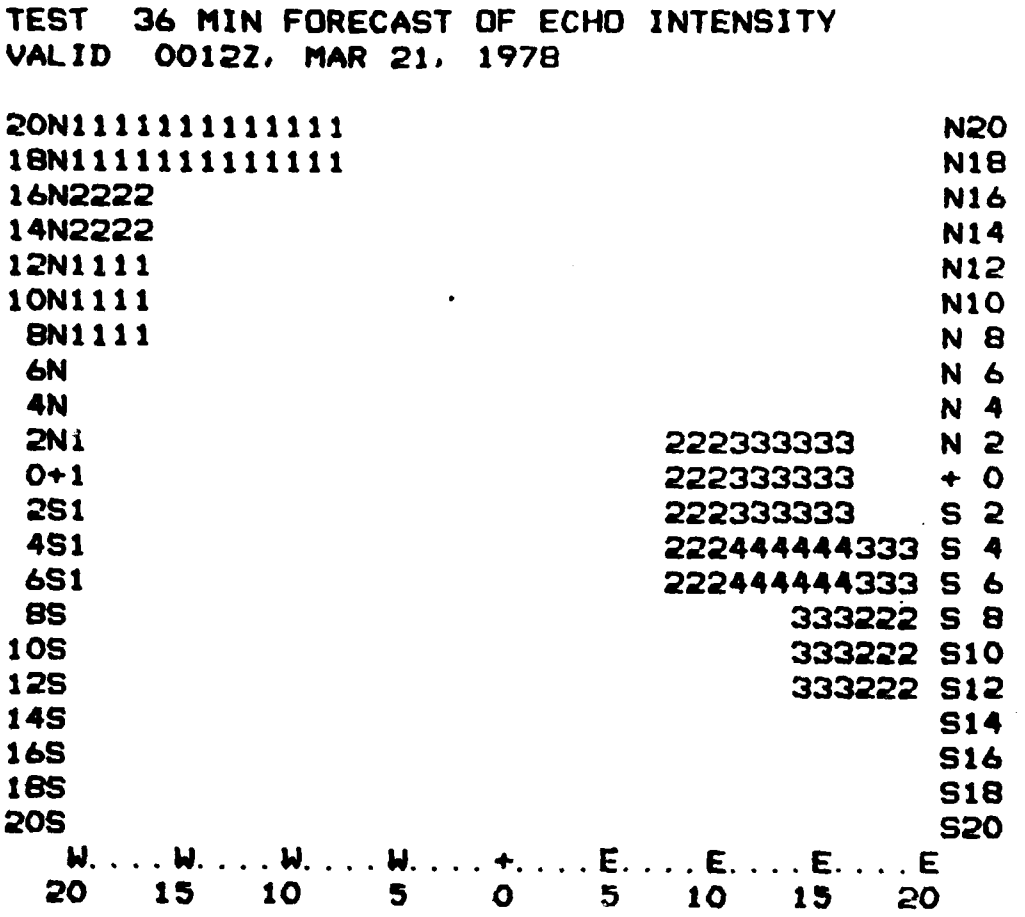

Figure 8. Mapped VIP values indicating the forecast ZTR intensities over a terminal area. In this case, the forecast is for 36 min and was made from data available at 2336 GMT.

REFERENCES

Alaka, M. A., J. P. Charba, and R. C. Elvander (1975). Short range thunderstorm forecasting for aviation. Interim Rep. to Federal Aviation Administration, Washington, D.C., Rep. No. FAA-RD-75-220, 24 pp.

Austin, G. L., and A. Bellon (1974). The use of digitial radar records for short term precipitation forecasting. Quart. J. Roy. Meteor. Soc., 100, pp. 33-39.

Blackmer, R. H., Jr., R. D. Duda, and R. Reboh (1973). Application of pattern recognition techniques to digitized weather radar data. Final Report Contract 1-3602, SRI Project 1287, Stanford Research Institute, Menlo Park, Calif., 89 pp.

Brandes, E. M. (1972). The use of digital radar in severe storm detection and prediction. Preprints 15th Radar Meteorology Conference, October 1972, Champaign-Urbana, Ill., Amer. Meteor. Soc., pp. 45-48.

Burgess, D. W., and D. R. Devore, (1979). Doppler radar utility in severe weather warnings. Preprints Eleventh Conference on Severe Local Storms, Amer. Meteor. Soc., Boston Mass., pp. 577-579.

Donaldson, R. J., Jr., R. M. Dyer, and M. J. Kraus, (1975). An objective evaluator of techniques for predicting severe weather events. Preprints Ninth Conference on Severe Local Storms, Amer. Meteor. Soc., Boston, Mass., pp. 321-326.

Elvander, R. C. (1976). An evaluation of the relative performance of three weather radar echo forecasting techniques. Preprints 17th Radar Meteorology Conference, October 1976, Seattle, Wash., Amer. Meteor. Soc., pp. 526-532.

_____, (1977). Relationships between radar parameters observed with objectively defined echoes and reported severe weather occurrences. Preprints 10th Conference on Severe Local Storms, October 1977, Omaha, Nebr., Amer. Meteor. Soc., pp. 73-76.

Greene, D. R. (1972). Vertically integrated liquid water - a new analysis tool. Mon. Wea. Rev., 100, pp 548-552.

Lemon, L. R. (1977). Severe thunderstorm evolution: its use in a new technique for radar warning. Preprints 10th Conference on Severe Local Storms, October 1977, Omaha, Nebr., Amer. Meteor. Soc., pp. 77-80.

McGrew, R. G.(1972). Project D/RADEX (Digitized Radar Experiments). Preprints 15th Radar Meteorology Conference, October 1972, Champaign-Urbana, Ill., Amer. Meteor. Soc., pp. 101-106.

Miller, R. G. (1958). The screening procedure. Studies in Statistical weather prediction. Final Report, Contract No. AF19 (604) - 1590. The Travelers Research Center, Inc., Hartford, Conn., pp. 86-95.

Palmer, W. C., and R. A. Allen (1949). Note on accuracy of forecast concerning the rain problem. Unpublished manuscript, U.S. Weather, Bureau, Washington, D.C., 4 pp.

Panofsky, H. A., and G. W. Brier, (1958). Some applications of statistics to meteorology. The Pennsylvania State University, University Park, Pa., 224 pp.

Saffle, R. E. (1976). D/RADEX products and field operation. Preprints 17th Radar Meteorology Conference, October 1976, Seattle, Wash., Amer. Meteor. Soc., pp. 555-559.

Wilson, J. W. (1971). Severe storm identification with the WSR-57. Preprints 7th Conference on Severe Local Storms, October 1971, Kansas City, Mo., Amer. Meteor. Soc., pp. 60-62.

U.S. GOVERNMENT PRINTING OFFICE: 1980-634-780/687